Science of the Total Environment 692 (2019) 1037–1047

Contents lists available at ScienceDirect

Science of the Total Environment

journal homepage: www.elsevier.com/locate/scitotenv

Transcriptomic response to changing ambient phosphorus in the marine dinoflagellate *Prorocentrum donghaiense*

Shu-Feng Zhang [a], Chun-Juan Yuan [a], Ying Chen [a], Lin Lin [a], Da-Zhi Wang [a,b,*]

[a] State Key Laboratory of Marine Environmental Science/College of the Environment and Ecology, Xiamen University, Xiamen 361102, China
[b] Key Laboratory of Marine Ecology & Environmental Sciences, Institute of Oceanology, Chinese Academy of Sciences, Qingdao 266071, China

HIGHLIGHTS

- *P. donghaiensis* exploited diverse utilization strategies of organic P to adapt to low P environments.
- Endocytosis might be a key strategy for *P. donghaiense* to capture extracellular DOP under DIP-deficient condition.
- Transcriptomic responses of *P. donghaiense* to DIP and DOP-resupplements were significantly different.
- DOP provided both P and carbon sources for *P. donghaiense* and played central roles in bloom formation.

GRAPHICAL ABSTRACT

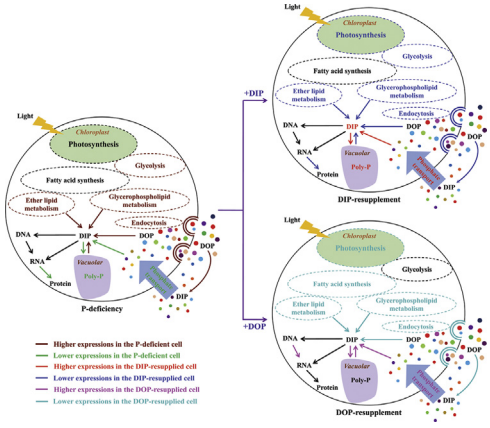

ARTICLE INFO

Article history:
Received 18 April 2019
Received in revised form 15 July 2019
Accepted 18 July 2019
Available online 19 July 2019

Editor: Jay Gan

Keywords:
Marine dinoflagellate
Harmful algal blooms
Prorocentrum donghaiense
Phosphorus
Transcriptomics

ABSTRACT

Dinoflagellates represent major contributors to the harmful algal blooms in the oceans. Phosphorus (P) is an essential macronutrient that limits the growth and proliferation of dinoflagellates. However, the specific molecular mechanisms involved in the P acclimation of dinoflagellates remain poorly understood. Here, the transcriptomes of a dinoflagellate *Prorocentrum donghaiense* grown under inorganic P-replete, P-deficient, and inorganic- and organic P-resupplied conditions were compared. Genes encoding low- and high-affinity P transporters were significantly down-regulated in the P-deficient cells, while organic P utilization genes were significantly up-regulated, indicating strong ability of *P. donghaiense* to utilize organic P. Up-regulation of membrane phospholipid catabolism and endocytosis provided intracellular and extracellular organic P for the P-deficient cells. Physiological responses of *P. donghaiense* to dissolved inorganic P (DIP) or dissolved organic P (DOP) resupply exhibited insignificant differences. However, the corresponding transcriptomic responses significantly differed. Although the expression of multiple genes was significantly altered after DIP resupplementation, few biological processes varied. In contrast, various metabolic processes associated with cell growth, such as translation, transport, nucleotide, carbohydrate and lipid metabolisms, were significantly altered in the DOP-resupplied cells. Our results indicated that *P. donghaiense* evolved diverse DOP utilization strategies to adapt to low P environments, and that DOPs might play critical roles in the *P. donghaiense* bloom formation.

* Corresponding author at: State Key Laboratory of Marine Environmental Science/College of the Environment and Ecology, Xiamen University, Xiamen 361102, China.
E-mail addresses: linlin1982@xmu.edu.cn (L. Lin), dzwang@xmu.edu.cn (D.-Z. Wang).

https://doi.org/10.1016/j.scitotenv.2019.07.291
0048-9697/

1. Introduction

Dinoflagellates are the major causative agents of harmful algal blooms (HABs), and are estimated to be responsible for >80% of the HABs in oceans worldwide (Wang, 2008; Wang et al., 2014; Lin et al., 2015; Gong et al., 2017; Morse et al., 2018). In the past few decades, the geographic distribution, frequency and scale of dinoflagellate-induced HABs have increased rapidly due to anthropogenic activities and global environmental changes, exerting severe impacts on marine ecosystem, mariculture and human health (Anderson et al., 2002; Edwards et al., 2006; Gobler et al., 2017; Gong et al., 2017; Xiao et al., 2017; Morse et al., 2018). For example, on the coastal Atlantic regions between 40°N and 60°N, potential mean annual growth rates and duration of the toxic dinoflagellates *Alexandrium fundyense* and *Dinophysis acuminata* blooms seasons significantly increased from 1982 to 2016 (Gobler et al., 2017). Consequently, the formation mechanisms of dinoflagellate blooms have become a hotspot in the field of HABs.

Multiple studies have indicated that the capabilities of dinoflagellates to respond to changing environments determine their success and proliferation, as well as blooms formation (Dyhrman, 2016; Gobler et al., 2017; Xiao et al., 2017). Phosphorus (P), an essential nutrient involved in various biochemical reactions and metabolic processes, such as cell membrane synthesis, signal transduction, photosynthesis, nucleic acid metabolism and energy metabolism (Takeda et al., 2006; Paytan and Mclaughlin, 2007; Wang et al., 2014; Dyhrman, 2016; Lin et al., 2016), greatly influences the growth and proliferation of dinoflagellates (White and Dyhrman, 2013; Zhang et al., 2014; Dyhrman, 2016; Lin et al., 2016; Zhang et al., 2018). However, the low concentrations of dissolved inorganic phosphorus (DIP) in many waters fail to meet the demand of dinoflagellates (Ou, 2008; Lin et al., 2011, 2012a, 2012b; Dyhrman, 2016; Lin et al., 2016). Phytoplankton have evolved diverse strategies to adapt to P-deficient environments (Dyhrman, 2016; Van Mooy et al., 2009; Zhang et al., 2016; Luo et al., 2017; Shi et al., 2017). Under P-replete conditions, some species such as *Thalassiosira pseudonana*, *Skeletonema costatum* and *Alexandrium catenella* can absorb and store large amounts of P as polyphosphate in their vacuoles, which is used when ambient P is deficient (Hothorn et al., 2009; Van Mooy et al., 2009; Jauzein et al., 2010; Orchard et al., 2010; Martin et al., 2011; Dyhrman et al., 2012; Fu et al., 2013; Zhang et al., 2016). Whereas, most species can increase the rates of P uptake/transportation, enhance the affinity of phosphate transporters, or utilize dissolved organic P (DOP), or membrane phospholipids or non-phospholipids (sulfolipid and betaine lipid) (Dyhrman et al., 2012; Dyhrman, 2016; Lin et al., 2016; Shi et al., 2017; Zhang et al., 2016; Zhang et al., 2019). Although DOP utilization by alkaline phosphatase (AP) has been reported (Dyhrman and Palenik, 2008; Lin et al., 2011, 2012a, 2012b; Dyhrman, 2016), the adaptive and response mechanisms of dinoflagellates to ambient P deficiency and resupplementation remain poorly understood.

P. donghaiensis is a representative dinoflagellate species responsible for the extensive HABs in the coastal East China Sea (Li et al., 2014; Lu et al., 2005; Huang et al., 2016; Yu et al., 2018), which severely impact the marine ecosystem and fisheries by reducing phytoplankton biodiversity and zooplankton abundance (Lin et al., 2014; Li et al., 2014; Huang et al., 2016; Zhou et al., 2017). The understanding of formation mechanisms of *P. donghaiense* bloom has been significantly improved (Li et al., 2014; Zhou et al., 2017), and P availability has been recognized as an essential factor regulating bloom formation (Zhang, 2012; Zhou et al., 2017). Notably, *P. donghaiense* is capable of forming large-scale and long-duration blooms even at very low ambient inorganic P concentrations (Zhou et al., 2017), implying that *P. donghaiense* may possess specialized P utilization strategies. Studies show that *P. donghaiense* can use DOPs, such as glucose 6-phosphate (G-6-P), ATP and RNA, to sustain growth under DIP-deficient conditions by employing AP (Huang et al., 2005; Ou, 2008; Ou et al., 2015; Zhang et al., 2018). However, comprehensive understanding of the molecular mechanisms involved in P acclimation is lacking (Zhang et al., 2018). In this study, the transcriptomes of *P. donghaiense* under P-replete, P-deficient, DIP-resupplied and DOP-resupplied conditions were compared and the differentially expressed genes were characterized. The goal of this study was to reveal the adaption strategy of *P. donghaiense* to ambient P deficiency and the response mechanisms to resupplementation of DIP or DOP.

2. Materials and methods

2.1. Culture conditions and experimental design

The *Prorocentrum donghaiense* was isolated from the East China Sea in May 2014 and was routinely maintained in K-medium at 20 °C under a 14 h:10 h light: dark cycle at a light intensity of approximately 100 μmol m^{-2} s^{-1} provided by fluorescent lamps (Ou et al., 2015; Zhang et al., 2015). Cells in the logarithmic growth phase were harvested using centrifugation (2500*g* for 15 min at 20 °C), washed twice with sterile seawater and inoculated in a fresh K-medium without P for two days to exhaust intracellular P, as described by Zhang et al. (2016).

The experiment included four treatments with an initial cell density of 8.0×10^3 cells mL^{-1} and triplicate biological replicates for each treatment. At the beginning of the experiment, medium with 10.0 μM and 0.2 μM Na_2HPO_4 were used for the P-replete and P-deficient cultures, respectively. At day 6, three P-deficient cultures were resupplied with Na_2HPO_4 to the final concentration of 10.0 μM and were assigned as the DIP-resupplied group, while another three P-deficient cultures were resupplied with G-6-P to the final concentration of 10.0 μM and were designated as the DOP-resupplied group. The cultures were regularly monitored for cell density, P concentration, particulate P (PP) content, bulk alkaline phosphatase activity (APA) and the photochemical efficiency of photosystem II (*Fv*/*Fm*), including samples collected at 4 h and 28 h after the resupply of DIP and DOP (Zhang et al., 2016).

2.2. Physiological analysis

Samples of each culture were collected at 11:00 am every day. The number of cells was manually counted under a light microscope. *Fv*/*Fm* was measured using PHYTO-PAM (Pulse Amplitude Modulation, ED, Walz, Effeltrich, Germany). The cultures (25 mL) were filtered with a GF/F membrane, and *P. donghaiense* cells retained on the membrane were used to determine PP content while the filtrates were used to determine DIP or DOP concentration. The membranes were first employed with 0.017 M magnesium sulfate ($MgSO_4$) and digested for 2 h (Jeffries et al., 1979). Then the PP content and DIP or DOP concentration were measured according to the phosphomolybdenum blue spectrophotometric method (Murphy and Riley, 1962; Jeffries et al., 1979). APA was fluorometrically measured based on the release of 3-*O*-methylfluorescein from 3-*O*-methylfluorescein phosphate (Sigma, USA) as reported by Ou et al. (2015). A Student's *t*-test was used to compare the difference of each parameter among the four treatments. A difference with p value <0.05 was considered statistically significant.

2.3. RNA extraction and sequencing

The P-replete cells in the exponential growth phase (day 4), the P-deficient cells at day 6, and the P-resupplied-4 h and the P-resupplied-28 h cells were harvested for transcriptomic analyses. Three biological replicates were collected for each treatment. Total RNA was extracted using the TRI Reagent (MRC, Cincinnati, OH, USA). The integrity of RNA was examined using a RNA Nano 6000 Assay Kit with the 2100 Bioanalyzer RNA Nanochip (Agilent Technologies, Santa Clara, CA, USA). Paired-end cDNA libraries were constructed using random

oligonucleotides, SuperScript II reverse transcriptase (Life Technologies, Carlsbad, CA, USA), DNA polymerase I (DNAP I; New England BioLabs) and RNase H (Invitrogen). Libraries were sequenced using the Illumina HiSeq™ 2000 platform (Expression Analysis Inc., San Diego, CA, USA).

2.4. De novo assembly, functional annotation and differential unigene expression analysis

High quality clean reads were obtained by quality control of the raw sequencing reads. Q20 of the clean reads in all samples were over 95%. De novo assembly was performed using the Trinity de novo assembler (Release-201302251, https://github.com/trinityrnaseq/trinityrnaseq/wiki) based on the high quality clean reads. The unigenes were annotated against the NCBI-NR (Release-20130408, Pruitt et al., 2005), NCBI-NT (Release-20130408, Pruitt et al., 2005), COG (Release-20090331, Tatusov et al., 2003), SwissProt (Release-63.0, UniProt, 2012) and KEGG (Release-63.0, Kanehisa and Goto, 2000) databases using BLAST (v2.2.26 + x64-linux). Unigene expression profiles were calculated based on the length of unigene and the number of reads mapped to the unigene (Mortazavi et al., 2008; Zhang et al., 2016). Differentially expressed genes (DEGs) were obtained by pairwise comparison with a false discovery rate ≦ 1% and a fold change ≧ 4 as the thresholds.

2.5. Validation of the DEGs using qRT-PCR

To validate the transcriptome results and DEGs, qRT-PCR analysis was performed using the ABI 7500 System (Applied Biosystems) with the SuperReal PreMix Plus (SYBR Green) Kit (Tiangen, China). Ten unigenes were selected for validation, and the specific primers for the selected unigenes were designed using the Primer Premier 5 software and listed in Table S1. The thermal cycle conditions were as follows: 50 °C for 2 min, 95 °C for 10 min, followed by 40 cycles of 95 °C for 30 s and 60 °C for 60 s. Calmodulin (*calm*) was used as an internal control because of its stable expression under different environmental conditions (Shi et al., 2015; Zhang et al., 2014; Zhang et al., 2016). The relative unigene expression levels were calculated based on the $2^{-\Delta\Delta Ct}$ relative response method (Zhang et al., 2014; Zhang et al., 2016).

2.6. Statistical analyses

All data in this study were analyzed using SPSS 17.0 (SPSS Inc., Chicago, IL, USA). Prior to analysis, data were tested for the equality of variances; p values <0.05 were considered statistically significant.

3. Results

3.1. Physiological responses of P. donghaiense to P variations

P. donghaiense cells of all treatments grew slowly in the first 2 days. From day 3 to 5, the P-replete cells proliferated rapidly and the cell density increased from 4.0×10^4 cells mL^{-1} to 1.2×10^5 cells mL^{-1}, followed by entry into the stationary phase at day 6 till day 10 (Fig. 1A). For the P-deficient cultures, cell proliferation ceased at an average cell density of 4.0×10^4 cells mL^{-1} from day 3 to 10. However, cell growth recovered immediately after resupplementation of Na_2HPO_4 or G-6-P at day 6, and the cell density of both groups exceeded 1.5×10^5 cells mL^{-1} at day 10 (Fig. 1A).

PP contents increased in both P-replete and -deficient cells as the P in the solution was rapidly absorbed at day 1 (Fig. 1B and C). From day 2 to day 5, the P concentration and PP content in the P-replete cells decreased with increasing cell density, and P was undetectable at day 5. However, bulk APA was very low from day 1 to 5, and increased slightly from day 6 to 10 (Fig. 1D). In the P-deficient cells, P was undetectable at day 2, PP content declined to a low level (Fig. 1B and C), and bulk APA was enhanced from day 3 (Fig. 1D). After 4 h of P resupply, P was exhausted in the Na_2HPO_4-resupplied cells and the concentration of P in the G-6-P-resupplied cells decreased rapidly from 10.0 μM to 2.5 μM. The PP content markedly increased after 4 h of P resupply, and then decreased (Fig. 1C). The bulk APA also declined rapidly after 4 h of P resupply, and remained stable from day 7 to day 9. However, the bulk APA was elevated again in both DIP and DOP-resupplied cells at day 10 (Fig. 1D).

Fv/*Fm* increased from day 0 to day 3 in both P-replete and -deficient cells (Fig. 1E). In the P-replete cells, *Fv*/*Fm* reached a peak value (around 0.6) at day 4 and then decreased gradually until around 0.2 at day 10 (Fig. 1E). Whereas, it decreased from day 4 to the end of the experiment in the P-deficient cells. After P resupplementation at day 6, *Fv*/*Fm* increased from day 7 to day 8, followed by decline at day 9 (Fig. 1E).

3.2. Sequencing, de novo assembly and functional annotation

Qualified cDNA libraries were sequenced using the Illumina HiSeq™ 2000 platform. After trimming and quality filtering, each data set of clean reads exhibited Q20 ≧ 95% with an average GC content of 63.11% (Table 1). All clean reads were submitted to the Sequence Read Archive database (BioProject ID: PRJNA522720). After de novo assembly with the Trinity software (https://github.com/trinityrnaseq/trinityrnaseq/wiki), 236,500 unigenes were generated with an average length of 936 bp and N50 of 1469 bp (Table 1), and 89,857 unigenes were longer than 1000 bp.

Overall, 138,691 (58.6%) unigenes were successfully annotated in at least one database (Table S1). Further functional analysis of the annotated unigenes by the KEGG and GO databases, respectively, revealed a high proportion of unigenes involved in transcription (63.51% to RNA transport and 60.14% to mRNA surveillance pathway, Fig. S1A), translation and expression (67.7% to translation, ribosomal structure and biogenesis, Fig. S1B).

3.3. Transcriptomic responses to P deficiency and DIP/DOP resupplementation

Of the 236,500 unigenes, 27,434 (11.6%) unigenes exhibited significant differences by pair-wise comparisons of the six treatments (Table S3). In the P-deficient cells, 1.8% of the unigenes were up-regulated and 0.3% were down-regulated compared with the P-replete cells (Fig. 2A). After P resupplement, the number of DEGs in the DOP-resupplied cells was higher than that in the DIP-resupplied cells, especially for the unigenes with up-regulated expression (Fig. 2A and B). Remarkably, only 2.1% and 5.3% of the DEGs were shared between the DIP- and DOP-resupplied cells after 4 h and 28 h of P supply (Fig. 2B).

P. donghaiense showed different responses to DIP- and DOP-resupplementation, 4 and 14 significantly enriched metabolic pathways were identified in the DIP- and DOP-resupplied cells, respectively (Table 2). DOP utilization (acid phosphatase, phospholipase D (*PLD*), protein phosphatase) and splicing (splicing factor) related unigenes were rapidly down-regulated after 4 h of DIP resupply, while unigenes encoding fatty acid synthesis (acetyl-CoA carboxylase) were first down-regulated after 4 h of DOP resupply (Table S4). Although the expression of many unigenes did not recover after 28 h of DIP and DOP resupply compared to the P-deficient cells, more unigenes including ATP synthesis related unigenes were down-regulated after 28 h of DIP and DOP resupply (Table S4).

No significantly enriched metabolic pathway was identified after 4 h of DIP-resupply, whereas 6 metabolic pathways associated with transcription, translation, carbohydrate metabolism and energy metabolism were significantly enriched after 28 h of DIP resupply (Table 2). However, 4 and 12 significantly enriched metabolic

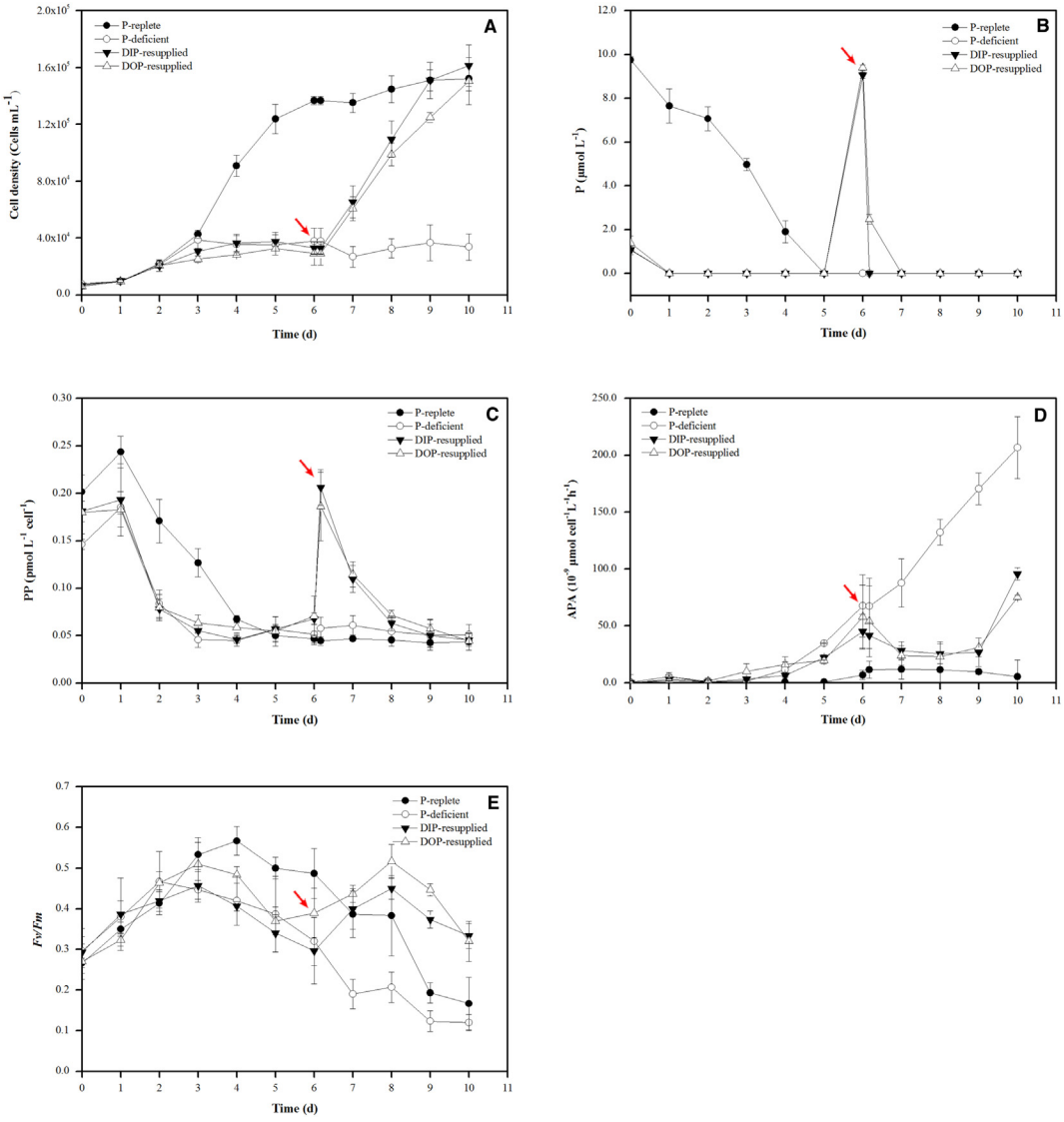

Fig. 1. Physiological responses of *P. donghaiense* to changing ambient P. (A) Cell density; (B) P concentration; (C) PP concentration; (D) APA; (E) *Fv*/*Fm*. PP, particulate organic phosphorus; APA, alkaline phosphatase activity; *Fv*/*Fm*, PSII maximum photochemical yield. The red arrow indicates the time of DIP (Na_2HPO_4) or DOP (G-6-P) resupplied. (For interpretation of the references to color in this figure legend, the reader is referred to the web version of this article.)

pathways were identified after 4 h and 28 h of DOP resupply, and these pathways were involved in carbohydrate metabolism, nucleotide metabolism, transcription, translation, lipid metabolism and energy metabolism (Table 2).

3.4. qRT-PCR validation of DEGs

To validate the RNA-Seq data, 10 DEGs were selected for RT-qPCR analysis. The expression levels of inorganic phosphate transporter (*PiT*),

Table 1
Overview of *P. donghaiense* transcriptome data.

Items	P-replete	P-deficient	DIP-resupplied-4 h	DOP-resupplied-4 h	DIP-resupplied-28 h	DOP-resupplied-28 h
Total raw reads	110,250,648	118,252,786	111,728,760	114,152,306	117,631,080	115,001,508
Total clean reads	102,871,212	110,160,396	103,162,608	105,550,656	108,828,594	106,655,688
Total clean nucleotides	9,258,409,080	9,914,435,640	9,284,634,720	9,499,559,040	9,794,573,460	9,599,011,920
Q20 percentage (%)	95.28	95.28	95.00	95.26	95.44	95.14
N percentage (%)	0.00	0.00	0.00	0.00	0.00	0.00
GC percentage (%)	63.64	63.96	63.45	61.94	62.65	63.05
Number of contigs	338,897	337,948	345,198	434,933	351,263	357,446
Number of unigenes	220,440	222,259	226,544	248,212	229,711	225,876

Total clean nucleotides = total clean Reads1 × Read1 size + total clean Reads2 × Read2 size. Q20 percentage is proportion of nucleotides with quality value larger than 20; N percentage is proportion of unknown nucleotides in clean reads; GC percentage is proportion of guanidine and cytosine nucleotides among total nucleotides.

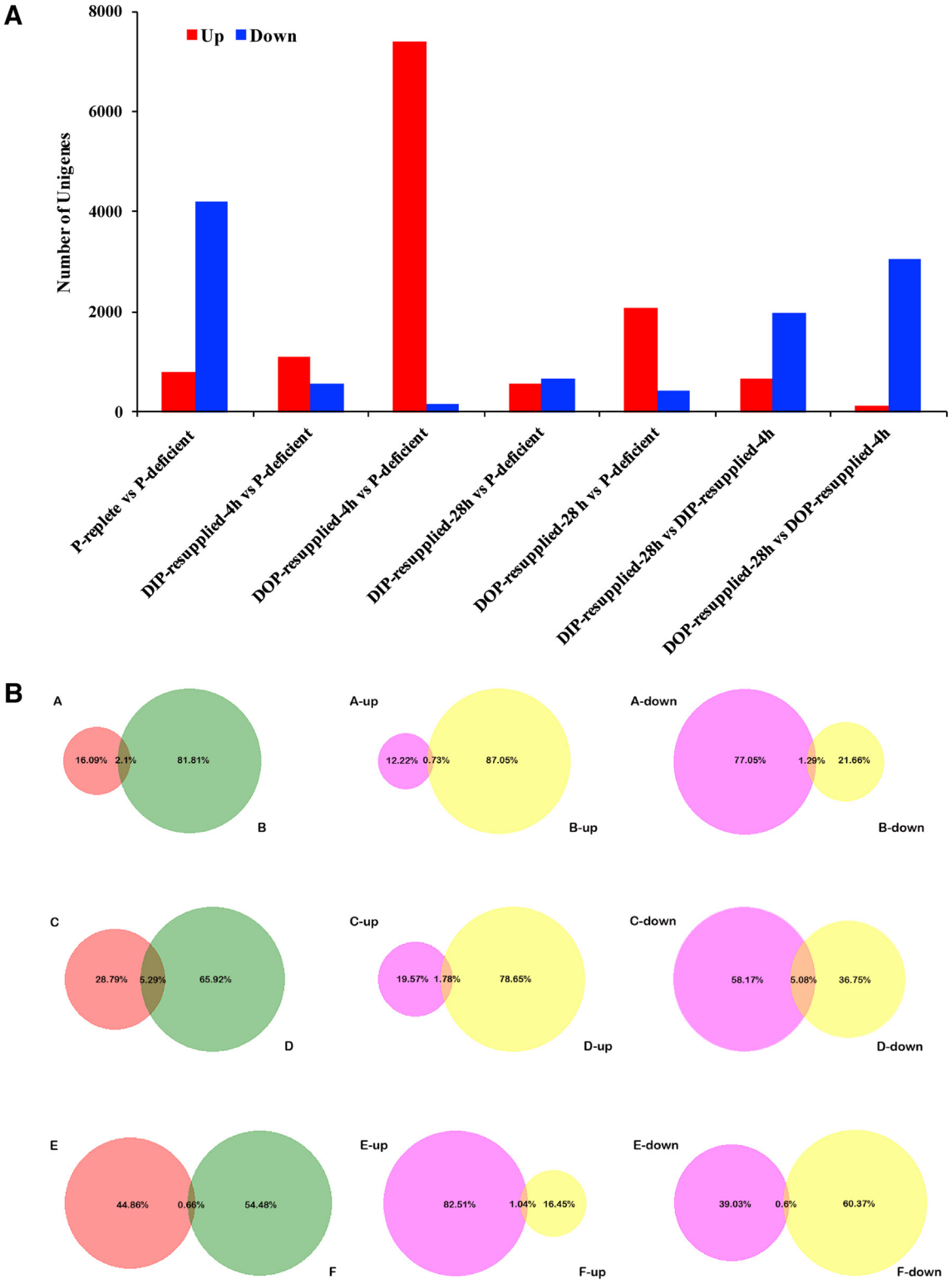

Fig. 2. Statistics of DEGs in *P. donghaiense* in response to P-depletion and P-resupplement. (A) Statistical analysis of DEGs in each comparison. "A vs B" is A normalized to B. (B) Comparison of DEGs in response of *P. donghaiense* to DIP- and DOP-resupplied. A: P-deplete vs DIP-4 h; B: P-deplete vs DOP-4 h; C: P-deplete vs DIP-28 h; D: P-deplete vs DOP-28 h; E: DIP-4 h vs DIP-28 h; F: DOP-4 h vs DOP-28 h. The size of the circle represents the number of DEGs.

high affinity phosphate transporter (*PHT*), alkaline phosphatase (*AP*), *PLD*, serine/arginine repetitive matrix protein 1 (*SRRM1*), RNA-binding protein with serine-rich domain 1 (*RNPS1*), 6-phosphofructokinase (*PFK1*), acetyl-CoA carboxylase (*ACC*), AP-2 complex subunit alpha (*AP2A2*) and dynamin GTPase (*Dyn GTPase*) were normalized with the reference gene calmodulin (*calm*). The expression patterns of *PiT*, *PHT*, *AP*, *PLD*, *SRRM1*, *AP2A2* and *Dyn GTPase* with P-replete, P-deficient, DIP- and DOP-resupplied treatments as determined by qRT-PCR were

Table 2
Metabolic processes with significant changes after DIP- and DOP-resupplement.

Pathway	DIP-resupplied-4 h vs P-deficient	DOP-resupplied-4 h vs P-deficient	DIP-resupplied-4 h vs DIP-resupplied-28 h	DOP-resupplied-4 h vs DOP-resupplied-28 h	Level 2
Propanoate metabolism	–	√	–	–	Carbohydrate metabolism
Pentose and glucuronate interconversions	–	√	–	√	
Starch and sucrose metabolism	–	√	–	√	
Pyrimidine metabolism	–	√	–	√	Nucleotide metabolism
Purine metabolism	–	√	–	√	
Spliceosome	–	√	√	√	Transcription
RNA polymerase	–	√	–	√	
Ribosome biogenesis in eukaryotes	–	√	–	√	Translation
RNA transport	–	–	√	–	
mRNA surveillance pathway	–	–	√	–	
Fatty acid biosynthesis	–	√	–	–	Lipid metabolism
Ether lipid metabolism	–	√	–	√	
Glycerophospholipid metabolism	–	√	–	√	
Synthesis and degradation of ketone bodies	–	√	–	–	
Oxidative phosphorylation	–	–	√	–	Energy metabolism
Endocytosis	–	√	–	√	Transport and catabolism
Base excision repair	–	–	–	√	Replication and repair
Zeatin biosynthesis	–	√	–	√	Metabolism of terpenoids and polyketides

"√" indicates that significantly enriched metabolic pathways; "–" indicates that no significantly enriched metabolic pathways.

consistent with those determined by RNA-seq, while only 4 of the 50 comparisons related to *RNPS1*, *PFK1* and *ACC* were inconsistent (Fig. 3). Moreover, the expression of most unigenes showed no statistically significant difference between the two data sets (*t*-test $p > 0.05$). These results suggested that on the whole, the RNA-Seq method provided a positive reference for the expression profiling study.

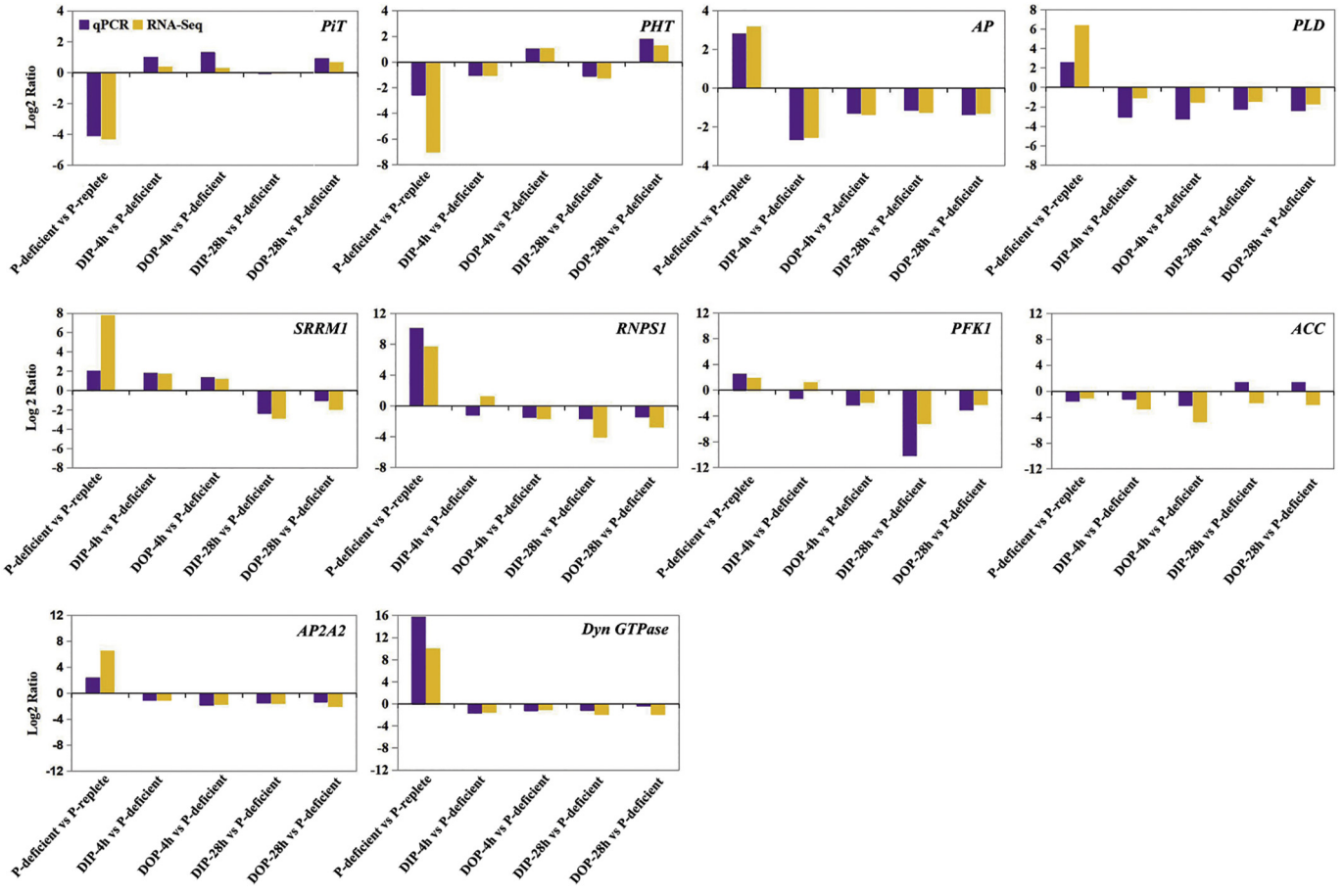

Fig. 3. qRT-PCR validations of DEGs. The housekeeping gene calm was chosen as the internal reference gene.

4. Discussion

4.1. Response mechanisms of P. donghaiense to ambient P deficiency

4.1.1. Phosphate transport

In contrast with many other phytoplankton species, phosphate transport in *P. donghaiense* was not enhanced but inhibited under the P-deficient condition. The transcriptional signal associated with P deficiency is not observed in the P-deficient *Karenia brevis*, despite rapid response of cell proliferation to P resupplementation (Morey et al., 2011). In addition, the expression level of phosphate transporters varies insignificantly in the proteome of the P-deficient *K. mikimotoi* (Lei and Lu, 2011). Phosphate is the preferred dissolved P source for phytoplankton (Dyhrman, 2016; Van Mooy et al., 2009). Under P-deficient conditions, many phytoplankton species increase phosphate uptake by up-regulating the expression of phosphate transporters at the transcription and/or protein level, such as the green algae *Chlamydomonas reinhardtii* (Moseley et al., 2006), the pelagophyte *Aureococcus anophagefferens* (Frischkorn et al., 2014), and the diatoms *Thalassiosira pseudonana* (Dyhrman et al., 2012), *Skeletonema* spp. (Alexander et al., 2015) and *S. costatum* (Zhang et al., 2016). However, expression of the proteins associated with phosphate uptake is down-regulated in the diatom *Phaeodactylum tricornutum* under P-deficient condition (Feng et al., 2014). In our study, the transcripts of 28 phosphate transporters, including 4 high-affinity phosphate transporters, 22 mitochondrial phosphate transporters and 47 sodium-dependent inorganic phosphate cotransporters, were identified in *P. donghaiense* (Table S5), indicating that *P. donghaiense* possesses high-affinity phosphate uptake systems. However, the expression of only 2 *PiT* and 4 *PHT* were significantly down-regulated in the P-deficient cells (Fig. 4), and no significant variation was detected after P resupplementation (Fig. 5), although P was quickly absorbed (Fig. 1B and Table S5). Therefore, dinoflagellates may possess other unknown phosphate transport mechanisms to achieve adaption to ambient P deficiency.

4.1.2. Phosphate homeostasis

Cellular inorganic phosphate levels can be sensed through the association of the Suppressor of Yeast gpa1/the yeast Phosphatase 81/the human Xenotropic and Polytropic Retrovirus receptor 1 (SPX) proteins with transcription factor domains triggered by inositol polyphosphate (Wild et al., 2016). SPX domain-containing proteins play critical roles in controlling eukaryotic cellular phosphate homeostasis, including inorganic phosphate uptake, transport, storage, membrane lipid remodeling and signaling systems (Secco et al., 2012; Wild et al., 2016). In the present study, the transcript level of SPX domain-containing membrane proteins was up-regulated by 2.5-fold under P-deficient condition, and no significant difference was observed 28 h after P resupplementation (Table S5). The expression of a unigene encoding SPX domain-containing proteins involved in vacuolar polyphosphate accumulation was down-regulated by 8.8-fold in the P-deficient cells and no significant variation occurred after P resupplementation (Table S5). *P. donghaiense* can store phosphate as intracellular polyphosphate in vacuoles when ambient P is well-supplied, similar to the diatoms *S. costatum* and *T. pseudonana* (Ou et al., 2008; Dyhrman et al., 2012; Zhang et al., 2016). Polyphosphate synthesis was suppressed in the P-deficient *P. donghaiense* (Fig. 4), and the excess P uptaken into the cells was not used for polyphosphate synthesis but for cell proliferation after P resupplementation (Fig. 5). Although the crucial role of polyphosphate is relatively clear, the mechanisms controlling its variability and metabolism are poorly understood (Secco et al., 2012). Our results suggested that intracellular P homeostasis was disrupted in the P-deficient *P. donghaiense* cells, and the intracellularly stored P was utilized.

4.1.3. Organic P utilization

Under DIP deficient conditions, DOP can serve as the major alternative P source for phytoplankton (Dyhrman et al., 2012; Ou et al., 2015; Zhang et al., 2016). APA is an indicator of DIP limitation, which is enhanced as the increase of limitation and is declined with the alleviation of limitation (Lin et al., 2012b). Under P deficiency, APA was markedly elevated accompanied by a significant up-regulation of AP transcript expression (Fig. 4). After P resupplementation, both the activity and transcript level of AP were significantly down-regulated in the P-resupplied-28 h cells (Fig. 5), while variations in the P-resupplied-4 h cells were not significant (Figs. 1D, 5 and Table S5). *P. donghaiense* can utilize exogenous phosphomonoester (G-6-P) (Fig. 4), similar to *K. brevis* (Morey et al., 2011), *S. costatum* and *T. pseudonana* (Dyhrman et al., 2012; Zhang et al., 2016). However, no significant difference was found in the utilization of the two P forms by these phytoplankton species. G-6-P is a low molecular weight phosphomonoester that can be readily hydrolyzed by AP (Ou et al., 2015; Zhang et al., 2016). Phospholipase A1 (PLA1) can hydrolyze membrane phospholipids and plays central roles in the maintenance and remodeling of cell membrane (Richmond and Smith, 2011). The transcript level of PLA1 showed a 5.9-fold increase in the P-deficient cells (Fig. 4), however, no significant change was found after P resupplementation (Fig. 5 and Table S5). The expression levels of the 75 unigenes of phosphodiesterase PLD were significantly up-regulated in the P-deficient cells (Fig. 4), while down-regulated in the P-resupplied-28 h cells (Fig. 5 and Table S5). PLD can hydrolyze assorted structural phospholipids, producing phosphatidic acid and various head groups (Zhao, 2015). Furthermore, PLD plays diverse roles in membrane transport, cell migration, hormone signaling and environmental stress response (Pleskot et al., 2013; Frohman, 2015; Zhao, 2015). PLD can also be recruited to the cell membrane in response to environmental and hormonal changes (Bargmann and Munnik, 2006). In addition, genes related to phospholipid metabolism, such as phospholipase A1, UDP-sugar pyrophosphorylase and acetylcholinesterase, were also identified with elevated expression levels in the P-deficient cells (Table S5). The expression levels of phospholipid-transporting ATPase genes were also significantly up-regulated under P deficiency and down-regulated after P resupplementation (Table S5). Phospholipid-transporting ATPase has been reported to produce phosphate via hydrolysis of phospholipids (Suzuki et al., 1997). Accordingly, under P deficiency, the utilization of intracellular phospholipids was enhanced in *P. donghaiense* (Fig. 4), and organic P became the major P source.

4.1.4. Endocytosis

Endocytosis plays essential roles in signal transduction, plasma membrane homeostasis, transport of extracellular materials into cells (such as nutrients, membrane proteins and lipids) and cellular response to environmental stimuli (Collinet et al., 2014; Fan et al., 2015). In eukaryotic cells, clathrin-mediated endocytosis is the major transport mechanism, and starts with the invagination of clathrin-coated membrane, through which extracellular molecules are packaged into clathrin-coated vesicles and taken up into the cells (Fan et al., 2015). The transcript expression levels of AP2 adaptor subunit alpha, Dyn GTPase and PLD were significantly up-regulated in the P-deficient cells and remarkably down-regulated in the DIP- or DOP-resupplied-28 h cells (Fig. 4, Tables S6 and S7). AP2 plays pivotal roles in the initiation of clathrin-coated pit nucleation (Fan et al., 2015). Dyn GTPase has been reported to regulate the formation of clathrin-coated vesicle and endocytic membrane fission (Warnock and Schmid, 1996; Ferguson and De Camilli, 2012). PLD activates Dyn GTPase and accelerates the endocytosis of epidermal growth factor receptor through its phox homology domain (Lee et al., 2006). The protein transport protein SEC24 is involved in vesicle trafficking as a component of the coat protein complex II (COPII), which promotes the emergence of transport vesicles from the endoplasmic reticulum (Pagano et al., 1999; Sucic et al., 2011). SEC24 is also needed for the first step of autophagosome formation, and its phosphorylation is known to regulate the abundance of autophagosomes during nutrient deprivation (Davis et al., 2017). In our study, the expression of protein transport protein SEC24 was also

significantly up-regulated under P deficiency and down-regulated after 28 h of P resupplementation (Figs. 4 and 5). Thus, endocytosis might be a key strategy for *P. donghaiense* to capture extracellular nutrients, including DIP and DOP, and to maintain intracellular homeostasis under DIP-deficient conditions (Fig. 4).

Although the expression profiles of many genes altered significantly in the P-deficient cells, these genes were only significantly enriched ($p \leqq 0.05$) in a few metabolic processes, such as ether lipid metabolism, glycerophospholipid metabolism and endocytosis (Fig. 4). The enhancement of phospholipid catabolism might provide an intracellular organic P source for *P. donghaiense* under P deficiency, while endocytosis not only provided a source of P, but also transported extracellular nitrogen and carbon sources into cells (Fig. 4). Therefore, although cell proliferation was suppressed due to P deficiency, the cells could survive. Compared with other phytoplankton species, *P. donghaiense* might have evolved particularly strong capabilities of organic P utilization.

4.2. Differential responses of P. donghaiense to resupplementation of DIP or DOP

In order to study the immediate response of *P. donghaiense* to different forms of P sources, the physiological and transcriptomic responses after 4 h and 28 h of DIP- and DOP-resupplementation were compared. Although the physiological responses of *P. donghaiense* to DIP- or DOP-resupplementation did not differ significantly, these were significantly different at the transcriptional level. After 4 h of P resupply, the key genes of the P directly requiring processes such as organic P utilization and RNA splicing in the DIP-resupplied-4 h cells were firstly down-regulated, but no change was found in the DOP-resupplied-4 h cells, this might be because DIP was more easily used than DOP (Table S4). Genes related to energy metabolism and RNA splicing began to recover after 28 h of P resupplementation (Table S4). Further analysis of metabolic pathways indicated that various biological processes, such as carbohydrate metabolism, lipid metabolism, nucleotide metabolism and transcription, were altered significantly after 4 h and/or 28 h of DOP resupplementation compared with the P deficient cells, while only the processes of spliceosome, RNA transport, mRNA surveillance pathway, glycolysis, photosynthesis and oxidative phosphorylation varied significantly in the DIP-resupplied-28 h cells (Table 2).

4.2.1. RNA transport and mRNA surveillance pathway

After transcription termination, the alternative splicing of mRNA precursors serves as a crucial mechanism for controlling gene expression, generating protein diversity, and ultimately affecting the shape and function of the *Arabidopsis* and rice (Syed et al., 2012). In *P. donghaiense*, the expression of splicing factors and serine/arginine repetitive matrix protein 1 was down-regulated under P-deficient condition (Fig. 4) and up-regulated 28 h after resupplementation of DIP (Fig. 5 and Table S7). Splicing factors are involved in the removal of introns from strings of messenger RNA, while the serine/arginine-rich proteins, which shuttle between the nucleus and cytoplasm, not only affect RNA splicing, but also play key roles in regulating mRNA translocation, mRNA stability and protein translation (Ali et al., 2007). The phosphorylation of serine/arginine-rich proteins strongly influences their mobility, which affects their recognition of precursor RNA, assembly of splicing complexes and splicing catalysis (Misteli et al., 2000). However, the expression levels of these genes did not change significantly in the DOP-resupplied group (Table 2). These results suggested that the RNA metabolism process that directly requires P was more sensitive to DIP than DOP, which could be due to the fact that DIP was more readily available than DOP.

4.2.2. Carbohydrate metabolism

Almost all plants can convert glucose or other polysaccharides to pyruvic acid via glycolysis, releasing ATP and reducing power (Plaxton, 1996). Moreover, the metabolic intermediates are also

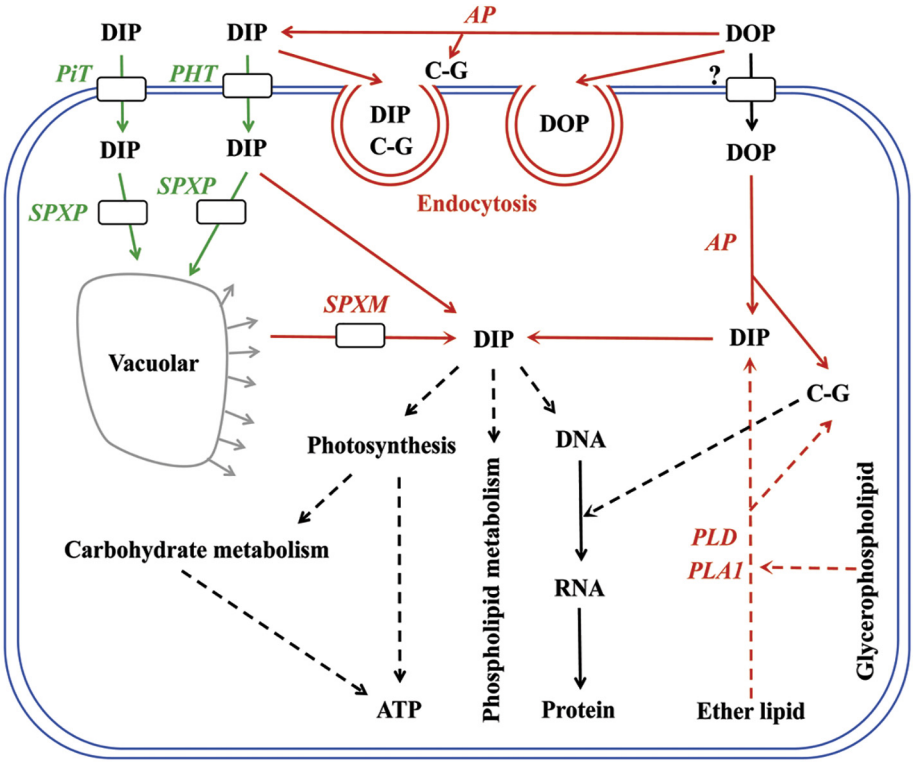

Fig. 4. P utilization strategies of *P. donghaiense* under P deficiency condition. C-G represents the carbon containing group after degradation of organic P. Red lines indicate that the process is up-regulated in the P-deficient cells, and green lines indicate that the process is down-regulated. AP: alkaline phosphatase; PLA1: phospholipase A1; PLD: phospholipase D; PHT: high affinity phosphate transporter; PiT: inorganic phosphate transporter; SPXM: SPX domain-containing membrane protein; SPXP: SPX domain-containing protein involved in vacuolar polyphosphate accumulation. (For interpretation of the references to color in this figure legend, the reader is referred to the web version of this article.)

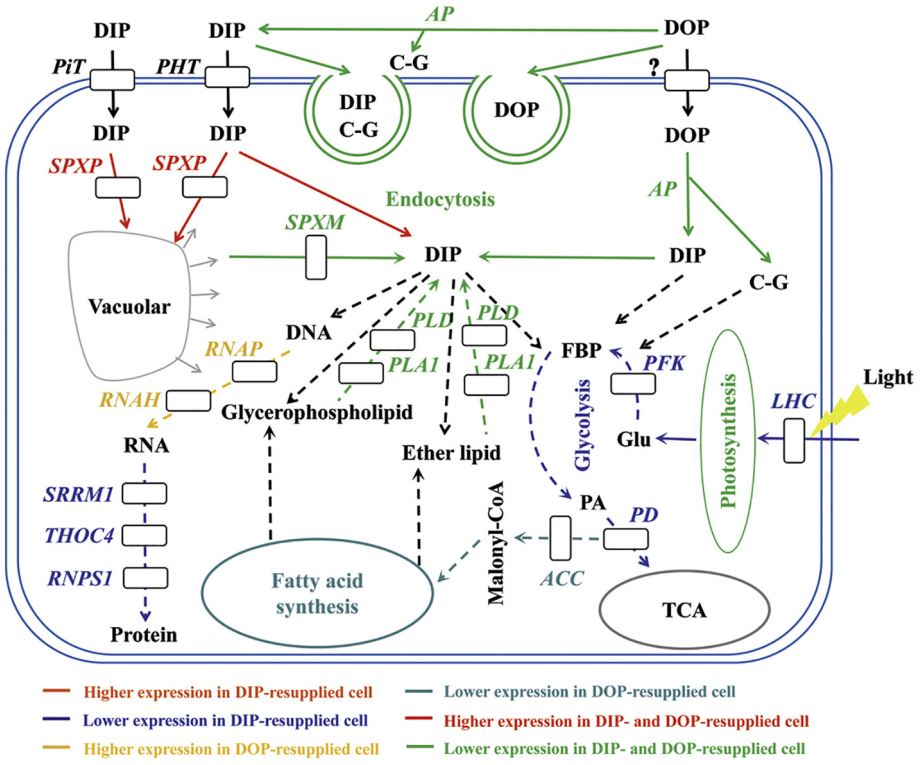

Fig. 5. Responses of *P. donghaiense* to DIP and DOP resupplementation. C-G represents the carbon containing group after degradation of organic P. ACC: acetyl-CoA carboxylase; AP: alkaline phosphatase; FBP: 1,6-fructose diphosphate; Glu: glucose; LHC: light-harvesting complex; PA: pyruvate; PD: pyruvate dehydrogenase; PFK: 6-phosphofructokinase; PHT: high affinity phosphate transporter; PiT: inorganic phosphate transporter; PLA1: phospholipase A1; PLD: phospholipase D; RNAH: RNA helicase; RNAP: RNA polymerase; RNPS1: RNA-binding protein with serine-rich domain 1; SPXM: SPX domain-containing membrane protein; SRRM1: serine/arginine repetitive matrix protein 1; SPXP: SPX domain-containing protein involved in vacuolar polyphosphate accumulation; THOC4: THO complex subunit 4.

precursors for the synthesis of cellular components such as amino acids and lipids (Kamp, 2013; Igamberdiev and Kleczkowski, 2018). In our study, the expression levels of PFK1 and pyruvate dehydrogenase (PD) were significantly down-regulated 28 h after resupplementation of DIP (Fig. 5 and Table S7). PFK1 is involved in the rate-limiting step of glycolysis, and directly controls the flow of carbon into the glycerol synthesis pathway via glycolysis (Teslaa and Teitell, 2014). PD, a key enzyme involved in cellular glucose metabolism, contributes to linking the glycolysis metabolic pathway to the citric acid cycle and releasing energy via NADH (Teslaa and Teitell, 2014). The down-regulation of PFK1 and PD expression 28 h after DIP resupplementation indicated that the cells required additional energy to activate the diverse defense mechanisms in responses to P deficiency, and that intracellular energy supply started to recover after resupply of DIP (Fig. 5 and Table S7). *Fv*/*Fm* is a potential valuable indicator of photoinhibition and nutrient limitation of phytoplankton (From et al., 2014). *Fv*/*Fm* decreased under P deficiency and increased after P resupplementation (Fig. 1E), however, the expression of light-harvesting complex (LHC) gene showed an opposite trend (Table S7). Gene encoding LHC was significantly down-regulated in the DIP-resupplied-28 h cells (Fig. 5 and Table S7). The LHC functions as a light-harvesting antenna that captures and transmits light energy to the reaction center, converting the light energy into chemical energy available to the plants (Okunlola and Adelusi, 2014). Nutrient stress can damage LHC and reduce its energy transfer rate, resulting in insufficient excitation energy in the reaction center and ultimately leading to the decrease of LHC energy conversion efficiency (Okunlola and Adelusi, 2014; Vidhyavathi et al., 2008). After DIP resupply, the cellular P stress was relieved and the transmission rate of LHC was restored (Fig. 5). Therefore, additional LHC transcripts were not required by the cells. However, no significant change was observed in the expression of these genes after DOP resupply, further supporting the point that DIP was preferentially used by *P. donghaiense* over DOP (Fig. 5). Our results indicated that DIP was more conducive to the recovery of intracellular energy production than DOP, as DIP provided P source more directly.

4.2.3. Transcription

Gene expression consists of three main stages regulated by RNA polymerase, spliceosome and ribosome, respectively. RNA polymerase is an enzyme responsible for copying the genetic information encoded in DNA to RNA during the transcription process (Onodera et al., 2005). In our study, the transcript level of the DNA-directed RNA polymerase II subunit RPB1, which controls the synthesis of mRNA from protein-coding genes, was significantly down-regulated in the P-deficient cells and up-regulated after DOP resupply (Figs. 4 and 5). However, no significant variation of RPB1 expression was observed in the DIP-resupplied cells (Fig. 5 and Table S7). In eukaryotic cells, spliceosomes are responsible for the removal of introns from transcribed pre-mRNAs, a class of primary transcripts (Will and Luhrmann, 2011). The transcript amounts of pre-mRNA-splicing factor ATP-dependent RNA helicase PRP16, ATP-dependent RNA helicase DHX8/PRP22 and ATP-dependent RNA helicase DDX46/PRP5 significantly decreased under P-deficient condition and significantly increased after DOP resupply (Table S7). It is reported that the transcription of *Trichoderma* spp. is regulated by certain carbon-metabolizing factors, such as carbon catabolite repression 1, and this process is also regulated by the ambient nutrient level, which greatly impact the adaptation and competition of *Trichoderma* spp. (Portnoy et al., 2011). Our results showed that transcription was inhibited in the P-deficient *P. donghaiense* cells (Fig. 4) but recovered after resupplementation of DOP (Fig. 5), indicating that unlike DIP, DOP might also serve as an alternative carbon source for the cells. Further investigation is required to confirm this suspected role of DOP.

4.2.4. Lipid metabolism

ACC catalyzes the formation of malonyl-CoA, an essential substrate involved in the rate-limiting step of fatty acid synthesis. Moreover, ACC also strongly influences lipid storage and overall energy metabolism (Abu-Elheiga et al., 2001, 2003). After 4 h of DOP resupply, the expression of AAC gene significantly declined (Fig. 5 and Table S7). The expression levels of phospholipid metabolism-related genes were elevated after 4 h and 28 h of DOP resupply (Fig. 5 and Table S7), indicating that intracellular P could not fulfill the nutritional requirement of cells. Compared with the DOP-resupplied-4 h cells, the number of DEGs in the DOP-resupplied-28 h cells was significantly lower, indicating alleviation of P deficiency in the cells to a certain extent. However, no significant change was found in the DIP-resupplied cells, although DIP was rapidly consumed after 4 h of DIP resupply, indicating that DOP provided the cells with not only P source but also carbon source. In addition, the findings indicated that G-6-P could be absorbed into cells directly. Taken together, these results demonstrated that phospholipids provided an important P source for cells under ambient P-deficient condition (Fig. 4).

5. Conclusions

This study investigated the molecular responses of *P. donghaiense* to ambient P deficiency and resupply at the transcriptional level. The expression of genes encoding low- and high-affinity P transporters in *P. donghaiense* was significantly down-regulated under P-deficient condition, while the expression of genes involved in organic P utilization was significantly up-regulated, indicating the strong ability of *P. donghaiense* to utilize organic P. Cell membrane phospholipids could serve as a major P source for the P-deficient cells, while the enhancement of endocytosis allowed the cells to capture more extracellular organic P. Although the physiological responses of *P. donghaiense* to DIP and DOP resupplementation exhibited insignificant differences, a greater number of metabolic processes showing significant changes were observed in the DOP-resupplied cells than in the DIP-resupplied cells. DIP could more rapidly restore RNA splicing and replenish energy source in the P-deficient cells than DOP, whereas DOP provided cells with both P and carbon sources rapidly restore metabolic processes, such as carbohydrate metabolism, transcription and lipid metabolism. Moreover, P deficiency might inhibit carbon utilization in *P. donghaiensis*. Overall, our results indicated that *P. donghaiensis* exploited diverse utilization strategies of organic P to adapt to low P environments, and that DOPs might play central roles in the bloom formation of *P. donghaiensis*.

Supplementary data to this article can be found online at https://doi.org/10.1016/j.scitotenv.2019.07.291.

Author contributions

Da-Zhi Wang and Shu-Feng Zhang planned and designed the research. Chun-Juan Yuan, Ying Chen and Lin Lin performed experiments and analyzed data. Da-Zhi Wang and Shu-Feng Zhang wrote the manuscript.

Declaration of Competing Interest

All the authors declare that there are no conflicts of interests regarding this article.

Acknowledgments

We thank the National Key Research and Development Program of China (Project No. 2017YFC1404300) and the National Natural Science Foundation of China (Project No. 41230961, 41425021 and 41706131) for financial support. Da-Zhi Wang is also supported by the 'Ten-thousand Talents Program' for leading talents in science and technological innovation.

References

Abu-Elheiga, L., Matzuk, M.M., Abo-Hashema, K.A.H., Wakil, S.J., 2001. Continuous fatty acid oxidation and reduced fat storage in mice lacking acetyl-CoA carboxylase 2. Science 291, 2613–2616.

Abu-Elheiga, L., Oh, W., Kordari, P., Wakil, S.J., 2003. Acetyl-CoA carboxylase 2 mutant mice are protected against obesity and diabetes induced by high-fat/high-carbohydrate diets. Proc. Natl. Acad. Sci. U. S. A. 100, 10207–10212.

Alexander, H., Jenkins, B.D., Rynearson, T.A., Dyhrman, S.T., 2015. Metatranscriptome analyses indicate resource partitioning between diatoms in the field. Proc. Natl. Acad. Sci. U. S. A. 112, E2182–E2190.

Ali, G.S., Palusa, S.G., Golovkin, M., Prasad, J., Manley, J.L., Reddy, A.S., 2007. Regulation of plant developmental processes by a novel splicing factor. PLoS One 2, e471.

Anderson, D.M., Glibert, P.M., Burkholder, J.M., 2002. Harmful algal blooms and eutrophication: nutrient sources, composition, and consequences. Estuaries 25, 704–726.

Bargmann, B.O., Munnik, T., 2006. The role of phospholipase D in plant stress responses. Curr. Opin. Plant Biol. 9, 515–522.

Collinet, C., Stöter, M., Bradshaw, C.R., Samusik, N., Rink, J.C., Kenski, D., et al., 2014. Systems survey of endocytosis by multiparametric image analysis. Nature 464, 243–249.

Davis, S., Wang, J., Ferronovick, S., 2017. Crosstalk between the secretory and autophagy pathways regulates autophagosome formation. Dev. Cell 41, 23–32.

Dyhrman, S.T., 2016. Nutrients and their acquisition: phosphorus physiology in microalgae. The Physiology of Microalgae. Springer International Publishing.

Dyhrman, S.T., Palenik, B.P., 2008. The identification and purification of a cell-surface alkaline phosphatase from the dinoflagellate *Prorocentrum minimum* (Dinophyceae). J. Phycol. 33, 602–612.

Dyhrman, S.T., Jenkins, B.D., Rynearson, T.A., Saito, M.A., Mercier, M.L., Alexander, H., et al., 2012. The transcriptome and proteome of the diatom *Thalassiosira pseudonana* reveal a diverse phosphorus stress response. PLoS One 7, e33768.

Edwards, M., Johns, D.G., Leterme, S.C., Svendsen, E., Richardson, A.J., 2006. Regional climate change and harmful algal blooms in the northeast Atlantic. Limnol. Oceanogr. 51, 820–829.

Fan, L.S., Li, R.L., Pan, J.W., Ding, Z.J., Lin, J.X., 2015. Endocytosis and its regulation in plants. Trends Plant Sci. 20, 388–397.

Feng, T.Y., Yang, Z.K., Zheng, J.W., Xie, Y., Li, D.W., Murugan, S.B., et al., 2014. Examination of metabolic responses to phosphorus limitation via proteomic analyses in the marine diatom *Phaeodactylum tricornutum*. Sci. Rep. 5.

Ferguson, S.M., De Camilli, P., 2012. Dynamin, a membrane-remodelling GTPase. Nat. Rev. Mol. Cell Biol. 13, 75–88.

Frischkorn, K.R., Harke, M.J., Gobler, C.J., Dyhrman, S.T., 2014. De novo assembly of *Aureococcus anophagefferens* transcriptomes reveals diverse responses to the low nutrient and low light conditions present during blooms. Front. Microbiol. 5, 375.

Frohman, M.A., 2015. The phospholipase D super family as therapeutic targets. Trends Pharmacol. Sci. 36, 137–144.

From, N., Richardson, K., Mousing, E.A., Jensen, P.E., 2014. Removing the light history signal from normalized variable fluorescence (Fv/Fm) measurements on marine phytoplankton. Limnol. Oceanogr. Meth. 12, 776–783.

Fu, M., Song, X.X., Yu, Z.M., Liu, Y., 2013. Responses of phosphate transporter gene and alkaline phosphatase in *Thalassiosira pseudonana* to phosphine. PLoS One 8, e59770.

Gobler, C.J., Doherty, O.M., Hattenrath-Lehmann, T.K., Griffith, A.W., Kang, Y., aLitaker, R.W., 2017. Ocean warming since 1982 has expended the niche of toxic algal blooms in the North Atlantic and North Pacific oceans. Proc. Natl. Acad. Sci. U. S. A. 114, 4975–4980.

Gong, W., Browne, J., Hall, N., Schruth, D., Paerl, H., Marchetti, A., 2017. Molecular insights into a dinoflagellate bloom. ISME J. 11, 439–452.

Hothorn, M., Neumann, H., Lenherr, E.D., Wehner, M., Rybin, V., Hassa, P.O., et al., 2009. Catalytic core of a membrane-associated eukaryotic polyphosphate polymerase. Science 324, 513–516.

Huang, B.Q., Ou, L.J., Hong, H.S., Luo, H., Wang, D.Z., 2005. Bioavailability of dissolved organic phosphorus compounds to typical harmful dinoflagellate *Prorocentrum donghaiense* Lu. Mar. Pollut. Bull. 51, 838–844.

Huang, X.Z., Huang, B.Q., Chen, J.X., Liu, X., 2016. Cellular responses of the dinoflagellate *Prorocentrum donghaiense* Lu to phosphate limitation and chronological ageing. J. Plankton Res. 38, fbv112.

Igamberdiev, A.U., Kleczkowski, L.A., 2018. The glycerate and phosphorylated pathways of serine synthesis in plants: the branches of plant glycolysis linking carbon and nitrogen metabolism. Front. Plant Sci. 9, 984.

Jauzein, C., Labry, C., Youenou, A., Quéré, J., Delmas, D., Collos, Y., 2010. Growth and phosphorus uptake by the toxic dinoflagellate *Alexandrium catenella* (dinophyceae) in response to phosphate limitation. J. Phycol. 46, 926–936.

Jeffries, D.S., Dieken, F.P., Jones, D.E., 1979. Performance of the autoclave digestion method for total phosphorus analysis. Water Res. 13, 275–279.

Kamp, M.W.V.D., 2013. Triosephosphate Isomerase-Computational Studies. Springer, Berlin Heidelberg, pp. 2658–2659.

Kanehisa, M., Goto, S., 2000. Kegg: Kyoto encyclopaedia of genes and genomes. Nucleic Acids Res. 28, 27–30.

Lee, C.S., Kim, I.S., Park, J.B., Lee, M.N., Lee, H.Y., Suh, P.G., et al., 2006. The phox homology domain of phospholipase D activates dynamin GTPase activity and accelerates EGFR endocytosis. Nat. Cell Biol. 8, 477–484.

Lei, Q.Y., Lu, S.H., 2011. Molecular ecological responses of the dinoflagellate *Karenia mikimotoi* to phosphate stress. Harmful Algae 12, 39–45.

Li, H.M., Tang, H.J., Shi, X.Y., Zhang, C.S., Wang, X.L., 2014. Increased nutrient loads from the Changjiang (Yangtze) river have led to increased harmful algal blooms. Harmful Algae 39, 92–101.

Lin, X., Zhang, H., Huang, B.Q., Lin, S.J., 2011. Alkaline phosphatase gene sequence and transcriptional regulation by phosphate limitation in *Amphidinium carterae* (dinoflagellate). J. Phycol. 47, 1110–1120.

Lin, X., Zhang, H., Cui, Y.D., Lin, S.J., 2012a. High sequence variability, diverse subcellular localizations, and ecological implications of alkaline phosphatase in dinoflagellates and other eukaryotic phytoplankton. Front. Microbiol. 3, 235.
Lin, X., Zhang, H., Huang, B.Q., Lin, S.J., 2012b. Alkaline phosphatase gene sequence characteristics and transcriptional regulation by phosphate limitation in *Karenia brevis* (Dinophyceae). Harmful Algae 17, 14–24.
Lin, J.N., Yan, T., Zhang, Q.C., Wang, Y.F., Liu, Q., Zhou, M.J., 2014. In situ detrimental impacts of *Prorocentrum donghaiense* blooms on zooplankton in the East China Sea. Mar. Pollut. Bull. 88 (1–2), 302–310.
Lin, S., Cheng, S., Song, B., Zhong, X., Lin, X., Li, W., et al., 2015. The *Symbiodinium kawagutii* genome illuminates dinoflagellate gene expression and coral symbiosis. Science 350, 691–694.
Lin, S.J., Litaker, R.W., Sunda, W.G., 2016. Phosphorus physiological ecology and molecular mechanisms in marine phytoplankton. J. Phycol. 52, 10–36.
Lu, D.D., Goebel, J., Qi, Y.Z., Zou, J.Z., Han, X.T., Gao, Y.H., et al., 2005. Morphological and genetic study of *Prorocentrum donghaiense* Lu from the East China Sea, and comparison with some related *Prorocentrum* species. Harmful Algae 4, 493–505.
Luo, H., Lin, X., Li, L., Zhang, C., Lin, S.J., 2017. Transcriptomic and physiological analyses of the dinoflagellate *Karenia mikimotoi* reveal non-alkaline phosphatase-based molecular machinery of ATP utilization. Environ. Microbiol 19, 4506–4518.
Martin, P., Van Mooy, B.A.S., Heithoff, A., Dyhrman, S.T., 2011. Phosphorus supply drives rapid turnover of membrane phospholipids in the diatom *Thalassiosira pseudonana*. ISME J. 5, 1057–1060.
Misteli, T., Gunjan, A., Hock, R., Bustin, M., Brown, D.T., 2000. Dynamic binding of histone H1 to chromatin in living cells. Nature 408, 877–881.
Morey, J.S., Monroe, E.A., Kinney, A.L., Beal, M., Johnson, J.G., Hitchcock, G.L., et al., 2011. Transcriptomic response of the red tide dinoflagellate, *Karenia brevis*, to nitrogen and phosphorus depletion and addition. BMC Genomics 12, 346.
Morse, D., Tse, S.P.K., Lo, S.C.L., 2018. Exploring dinoflagellate biology with high-throughput proteomics. Harmful Algae 27, 31–36.
Mortazavi, A., Williams, B.A., McCue, K., Schaeffer, L., Wold, B., 2008. Mapping and quantifying mammalian transcriptomes by RNA-Seq. Nat. Methods 5, 621–628.
Moseley, J.L., Chang, C.W., Grossman, A.R., 2006. Genome-based approaches to understanding phosphorus deprivation responses and PSR1 control in *Chlamydomonas reinhardtii*. Eukaryot. Cell 5, 26–44.
Murphy, J., Riley, J.P., 1962. A modified single solution method for the determination of phosphate in natural waters. Anal. Chim. Acta 27, 31–36.
Okunlola, G.O., Adelusi, A.A., 2014. Growth and photosynthetic pigment accumulation in *Lycopersicum esculentum* mill. In response to light and nutrient stress. P. Fin. Dent. Soc. Suomen Hammaslääkäriseuran 6, 109–112.
Onodera, Y., Haag, J.R., Ream, T., Nunes, P.C., Pontes, O., Pikaard, C.S., 2005. Plant nuclear RNA polymerase IV mediates siRNA and DNA methylation-dependent heterochromatin formation. Cell 120, 613–622.
Orchard, E.D., Benitez-Nelson, C.R., Pellechia, P.J., Lomas, M.W., Dyhrman, S.T., 2010. Polyphosphate in Trichodesmium from the low-phosphorus Sargasso Sea. Limnol. Oceanogr. 55, 2161–2169.
Ou, L.J., 2008. Ecophysiological Responses of Typical Harmful Algal Bloom Species to Phosphorus. Xiamen University, Xiamen, pp. 96–102.
Ou, L.J., Huang, X.Y., Huang, B.Q., Qi, Y.Z., Lu, S.H., 2015. Growth and competition for different forms of organic phosphorus by the dinoflagellate *Prorocentrum donghaiense* with the dinoflagellate *Alexandrium catenella* and the diatom *Skeletonema costatum* s. l. Hydrobiologia 754, 29–41.
Pagano, A., Letourneur, F., Garcia-Estefania, D., Carpentier, J.L., Orci, L., Paccaud, J.P., 1999. Sec24 proteins and sorting at the endoplasmic reticulum. J. Biol. Chem. 274, 7833–7840.
Paytan, A., Mclaughlin, K., 2007. The oceanic phosphorus cycle. Chem. Rev. 107, 563–576.
Plaxton, W.C., 1996. The organization and regulation of plant glycolysis. Annu. Rev. Plant Physiol. Plant Mol. Biol. 147, 185–214.
Pleskot, R., Li, J., Žárský, V., Potocký, M., Staiger, C.J., 2013. Regulation of cytoskeletal dynamics by phospholipase D and phosphatidic acid. Trends Plant Sci. 18, 496–504.
Portnoy, T., Margeot, A., Linke, R., Atanasova, L., Fekete, E., Sándor, E., et al., 2011. The CRE1 carbon catabolite repressor of the fungus *Trichoderma reesei*: a master regulator of carbon assimilation. BMC Genomics 12, 269.
Pruitt, K.D., Tatusova, T., Maglott, D.R., 2005. NCBI reference sequence (RefSeq): a curated non-redundant sequence database of genomes, transcripts and proteins. Nucleic Acids Res. 33, D501–D504.
Richmond, G.S., Smith, T.K., 2011. Phospholipases A1. Int. J. Mol. Sci. 12, 588.
Secco, D., Wang, C., Arpat, B.A., Wang, Z., Poirier, Y., Tyerman, S.D., et al., 2012. The emerging importance of the SPX domain-containing proteins in phosphate homeostasis. New Phytol. 193, 842–851.
Shi, X.G., Li, L., Guo, C.T., Lin, X., Li, M.Z., Lin, S.J., 2015. Rhodopsin gene expression regulated by the light dark cycle, light spectrum and light intensity in the dinoflagellate *Prorocentrum*. Front. Microbiol. 6, 555.
Shi, X.G., Lin, X., Li, L., Li, M.Z., Palenik, B., Lin, S.J., 2017. Transcriptomic and microRNAomic profiling reveals multi-faceted mechanisms to cope with phosphate stress in a dinoflagellate. ISME J. 11, 2209–2218.
Sucic, S., El-Kasaby, A., Kudlacek, O., Sarker, S., Sitte, H.H., Marin, P., et al., 2011. The serotonin transporter is an exclusive client of the coat protein complex II (COPII) component SEC24C. J. Biol. Chem. 286, 16482–16490.
Suzuki, H., Kamakura, M., Morii, M., Takeguchi, N., 1997. The phospholipid flippase activity of gastric vesicles. J. Biol. Chem. 272, 10429–10434.
Syed, N.H., Kalyna, M., Marquez, Y., Barta, A., Brown, J.W.S., 2012. Alternative splicing in plants-coming of age. Trends Plant Sci. 17, 616–623.
Takeda, E., Taketani, Y., Nashiki, K., Nomoto, M., Shuto, E., Sawada, N., et al., 2006. A novel function of phosphate-mediated intracellular signal transduction pathways. Adv. Enzym. Regul. 46, 154–161.
Tatusov, R.L., Fedorova, N.D., Jackson, J.D., Jacobs, A.R., Kiryutin, B., Koonin, E.V., et al., 2003. The COG database: an updated version includes eukaryotes. BMC Bioinforma. 4, 41.
Teslaa, T., Teitell, M.A., 2014. Chapter five-techniques to monitor glycolysis. Method. Enzymol. 542, 91–114.
UniProt, C., 2012. Reorganizing the protein space at the universal protein resource (UniProt). Nucleic Acids Res. 40, D71–D75.
Van Mooy, B.A.S., Fredricks, H.F., Pedler, B.E., Dyhrman, S.T., Karl, D.M., Koblížek, M., et al., 2009. Phytoplankton in the ocean use non-phosphorus lipids in response to phosphorus scarcity. Nature 458, 69–72.
Vidhyavathi, R., Venkatachalam, L., Sarada, R., Ravishankar, G.A., 2008. Regulation of carotenoid biosynthetic genes expression and carotenoid accumulation in the green alga *Haematococcus pluvialis* under nutrient stress conditions. J. Exp. Bot. 59, 1409–1418.
Wang, D.Z., 2008. Neurotoxins from marine dinoflagellates: a brief review. Mar. Drugs 6, 349–371.
Wang, D.Z., Zhang, H., Zhang, Y., Zhang, S.F., 2014. Marine dinoflagellate proteomics: current status and future perspectives. J. Proteome 105, 121–132.
Warnock, D.E., Schmid, S.L., 1996. Dynamin GTPase, a force-generating molecular switch. BioEssays News Rev. Mol. Cell. Dev. Biol. 18, 885–893.
White, A., Dyhrman, S.T., 2013. The marine phosphorus cycle. Front. Microbiol. 4, 105.
Wild, R., Gerasimaite, R., Jung, J.Y., Truffault, V., Pavlovic, I., Schmidt, A., et al., 2016. Control of eukaryotic phosphate homeostasis by inositol polyphosphate sensor domains. Science 352, 986–990.
Will, C.L., Luhrmann, R., 2011. Spliceosome structure and function. C. S. H. Perspect. Biol. 3, a003707.
Xiao, W., Liu, X., Irwin, A.J., Laws, E.A., Wang, L., Chen, B., et al., 2017. Warming and eutrophication combine to restructure diatoms and dinoflagellates. Water Res. 128, 206–216.
Yu, R.C., Lü, S.H., Liang, Y.B., 2018. Global Ecology and Oceanography of Harmful Algal Blooms Chap. 15. Springer.
Zhang, X., 2012. Historical Comparison on Evolution of Nutrient and Its Function on the Harmful Algae Blooms in Yangtze Estuary and Its Adjacent Sea. Ocean University of China, Qingdao.
Zhang, C., Lin, S.J., Huang, L.M., Wang, L., Li, M.Z., Liu, S., 2014. Suppression subtraction hybridization analysis revealed regulation of some cell cycle and toxin genes in *Alexandrium catenella* by phosphate limitation. Harmful Algae 39, 26–39.
Zhang, Y.J., Zhang, S.F., He, Z.P., Lin, L., Wang, D.Z., 2015. Proteomic analysis provides new insights into the adaptive response of a dinoflagellate Prorocentrum donghaiense to changing ambient nitrogen. Plant Cell Environ. 38, 2128–2142.
Zhang, S.F., Yuan, C.J., Chen, Y., Chen, X.H., Li, D.X., Liu, J.L., et al., 2016. Comparative transcriptomic analysis reveals novel insights into the adaptive response of *Skeletonema costatum* to changing ambient phosphorus. Front. Microbiol. 7, 1476.
Zhang, C.Y., Chen, G.F., Wang, Y.Y., Guo, C.L., Zhou, J., 2018. Physiological and molecular responses of *Prorocentrum donghaiense* to dissolved inorganic phosphorus limitation. Mar. Pollut. Bull. 129, 562–572.
Zhang, S.F., Chen, Y., Xie, Z.X., Zhang, H., Lin, L., Wang, D.Z., 2019. Unraveling the molecular mechanism of the response to changing ambient phosphorus in the dinoflagellate *Alexandrium catenella* with quantitative proteomics. J. Proteome 196, 141–149.
Zhao, J., 2015. Phospholipase D and phosphatidic acid in plant defence response: from protein–protein and lipid-protein interactions to hormone signalling. J. Exp. Bot. 66, 1721–1736.
Zhou, Z.X., Yu, R.C., Zhou, M.J., 2017. Seasonal succession of microalgal blooms from diatoms to dinoflagellates in the East China Sea: a numerical simulation study. Ecol. Model. 360, 150–162.